Radiation drag effects on magnetically dominated outflows around compact objects

V. S. Beskin, Nadia L. Zakamska, Hélène Sol

Mon. Not. R. Astron. Soc. **347,** 587–600 (2004)

Radiation drag effects on magnetically dominated outflows around compact objects

V. S. Beskin,[1⋆] N. L. Zakamska[2,3] and H. Sol[4]

[1]*P. N. Lebedev Physical Institute, Leninsky prosp., 53, Moscow 119991, Russia*
[2]*Department of Astrophysical Sciences, Princeton University, Princeton, NJ 08544, USA*
[3]*Moscow Institute of Physics and Technology, Dolgoprudny 141700, Russia*
[4]*LUTH, Observatory Paris-Meudon, Pl. J. Janssen 5, Meudon 92195, France*

Accepted 2003 September 22. Received 2003 September 21; in original form 2002 September 30

ABSTRACT

The effects of radiation drag force on the structure of relativistic electron–positron and electron–proton outflows are considered within the one-fluid approximation for a quasi-monopole cold outflow. It is shown that for a Poynting-dominated case, the drag force does not change the particle energy inside a fast magnetosonic surface. In this region, the action of the drag results in a diminution of the Poynting flux, not the particle flux. Outside the fast magnetosonic surface, for intermediate photon density, the drag force may result in additional acceleration of the plasma. This acceleration is the result of the disturbance of magnetic surfaces under the action of the drag. At even larger distances, particles are not frozen into the magnetic field and the drag force decelerates them efficiently.

In the case of extreme photon densities, the disturbance of magnetic surfaces becomes large and the drag force changes the total energy flux significantly, the particles becoming non-relativistic.

We find that for active galactic nuclei, the photon density is too low to disturb the parameters of an ideal magnetohydrodynamic outflow. The drag action may result in additional acceleration of outgoing plasma only for central engines with very high luminosities. For cosmological gamma-ray bursts, the drag force can strongly affect the process of formation of a Poynting-dominated outflow.

Key words: acceleration of particles – MHD – galaxies: active – gamma-rays: bursts.

1 INTRODUCTION

Magnetohydrodynamic (MHD) models are now developed intensively in theories concerning the magnetospheres of rotating supermassive black holes ($M \sim 10^8$–10^9 $M_\odot$, $B_0 \sim 10^4$ G), which are believed to reside in the central engines of active galactic nuclei (AGN) and quasars (Begelman, Blandford & Rees 1984; Thorne, Price & Macdonald 1986). In particular, it is the MHD model that is the most promising in the problem of the origin and stability of jets. Indeed, the MHD approach explains both the energy source (the rotational energy of the compact object) and the mechanism of the energy and angular momentum loss (for an overview, see e.g. Blandford 2002). Observational evidence in favour of MHD models was recently found in the possible presence of toroidal magnetic fields in jets (Gabuzda et al. 1992; Gabuzda, Pushkarev & Cawtorne 1999). Magnetically dominated outflows are also believed to be responsible for the energy transport in cosmological gamma-ray bursts (Mészáros & Rees 1997; Lee, Wijers & Brown 2000; van Putten & Levinson 2003), when energy is released in the merging of black holes or neutron stars ($M \sim M_\odot$, $B_0 \sim 10^{15}$ G).

It has been suggested that the density of photons in the vicinity of the central engine is so high that they may drastically change the characteristics of the ideal MHD outflow. For example, they may result in extensive e^+e^- pair creation (Svensson 1984), acceleration of low-energy pairs by the radiation drag force (Phinney 1982; Turolla, Nobili & Calvani 1986; Beloborodov 1999) and deceleration of high-energy particles (Melia & Königl 1989; Sikora et al. 1996). In other words, a self-consistent consideration should take the drag force into account.

So far the two processes (the ideal MHD acceleration and the action of external photons) have been considered independently. The first step to combine them was made by Li, Begelman & Chiueh (1992). In particular, it was shown how the equations can be integrated in a conical geometry (which is impossible in the general case). On the other hand, the consideration was performed within the approximation of

⋆E-mail: beskin@lpi.ru

a fixed poloidal magnetic field. Under this assumption the fast magnetosonic surface of a cold flow is shifted to infinity (Michel 1969; Kennel, Fujimura & Okamoto 1983; Lery et al. 1998). As a result, it was impossible to analyse the effects of radiation drag on the position of the fast magnetosonic surface and the properties of the outflow outside this surface.

The main goal of this paper is to determine more carefully the radiation drag effects on a magnetically dominated outflow. Here we consider a quasi-monopole outflow to analytically describe the effects of radiation drag, including simultaneously the disturbance of the magnetic surfaces. For AGN, such geometry in the immediate vicinity of the central engine was recently confirmed by direct observations (Junior, Biretta & Livio 1999). In other words, in the zeroth approximation (i.e. without drag) we use the analytical solution for a magnetically dominated MHD outflow (Beskin, Kuznetsova & Rafikov 1998, hereafter Paper I), in which the fast magnetosonic surface is located at a finite distance from the origin.

For simplicity we consider the following model of the radiation field in the vicinity of the central engine. First, we note that for ultrarelativistic particles the energy of a photon propagating nearly along the particle trajectory remains almost the same after a collision. This means that the drag force from these photons is small. Thus, only the isotropic component of the photon field contributes substantially to the drag force. Hence, in our geometry with a strong central source of photons and a monopole outflow of particles, only a small fraction of photons (the isotropic component of the photon field) interacts efficiently with the particles, producing inverse Compton photons with energies $\mathcal{E}_{\rm IC} \sim \gamma^2 \mathcal{E}_{\rm ph}$.

The isotropic component can be produced, first, by the outer part of the accretion disc and, secondly, by external sources. It can be modelled as

$$U = U_{\rm iso} = U_{\rm A}\left(\frac{r}{R_{\rm L}}\right)^{-n} + U_{\rm ext}, \tag{1}$$

where $R_{\rm L} = c/\Omega$ is the radius of the light cylinder, $U_{\rm A} = U(R_{\rm L}) = L_{\rm tot}/(4\pi\, R_{\rm L}^2 c)$ and $n \approx 3$ (for more details see, e.g., Sikora et al. 1996). Here the first term describes the radiation from the outer parts of the disc, $r_{\rm rad} > r$, while the second term corresponds to the homogeneous external radiation. For AGN this can be due to clouds located at a distance $r_{\rm cloud} \sim 1$ pc from the central engine and reradiating $kL_{\rm tot}$ of the total luminosity ($k \sim 10$ per cent). In this case

$$U_{\rm ext} = k\frac{L_{\rm tot}}{4\pi r_{\rm cloud}^2 c}. \tag{2}$$

However, this model only makes physical sense at distances less than $r_{\rm cloud}$, and the term vanishes at larger distances.

Finally, as some arguments exist both in favour of (Reynolds et al. 1996; Hirotani et al. 1999) and against (Sikora & Madejski 2000) the leading role of e^+e^- plasma in relativistic jets, in the following we consider both electron–positron and electron–proton outflows.

In Section 2 we formulate the basic equations describing a quasi-monopole outflow of relativistic plasma in two-fluid and one-fluid approximations. Then in Section 3 we analyse the main properties of an electron–positron outflow. A similar analysis for electron–proton plasma is produced in Section 4. Finally, in Section 5 we consider the effects of radiation drag for real astrophysical objects.

2 BASIC EQUATIONS

2.1 The two-fluid description

We consider an axisymmetric, stationary outflow of two-component cold plasma from the magnetosphere of a rotating body with a split monopole poloidal magnetic field. This geometry can be realized in the presence of an accretion disc separating the ingoing and outgoing magnetic fluxes (Blandford & Znajek 1977). In the hydrodynamic approximation, the structure of the flow is described by Maxwell's equations and the separate equations of motion for positively and negatively charged particles:

$$\begin{aligned}
&\nabla \boldsymbol{E} = 4\pi\rho_{\rm e}, \qquad \nabla \times \boldsymbol{E} = 0,\\
&\nabla \boldsymbol{B} = 0, \qquad \nabla \times \boldsymbol{B} = \frac{4\pi}{c}\boldsymbol{j},\\
&(\boldsymbol{v}^{\pm}\nabla)\boldsymbol{p}^{\pm} = \pm e\left(\boldsymbol{E} + \frac{\boldsymbol{v}^{\pm}}{c} \times \boldsymbol{B}\right) + \boldsymbol{F}^{\pm}_{\rm drag},
\end{aligned} \tag{3}$$

where $\boldsymbol{E}$ and $\boldsymbol{B}$ are the electric and magnetic fields, $\rho_{\rm e} = e(n^+ - n^-)$ and $\boldsymbol{j} = e(n^+\boldsymbol{v}^+ - n^-\boldsymbol{v}^-)$ are the charge and current densities, and $\boldsymbol{v}^{\pm}$ and $\boldsymbol{p}^{\pm}$ are the velocities and momenta of the charged particles. Finally, $\boldsymbol{F}^{\pm}_{\rm drag}$ are the radiation drag forces which, for an isotropic photon field, have the form

$$\boldsymbol{F}^{\pm}_{\rm drag} = -\frac{4}{3}\frac{\boldsymbol{v}^{\pm}}{|\boldsymbol{v}^{\pm}|}\left(\frac{m_{\rm e}}{m_{\pm}}\right)^2 \sigma_{\rm T} U_{\rm iso}(\gamma^{\pm})^2, \tag{4}$$

where $\gamma^{\pm}$ are the Lorentz factors, m_+ is the mass of the positively charged particles (positrons or protons) and $m_- = m_{\rm e}$ is the mass of the negatively charged particles. $\sigma_{\rm T} = (8\pi/3)(e^2/m_{\rm e}c^2)^2$ is the Thompson cross-section. To close system (3) the continuity equations $\nabla\,(n^{\pm}\,\boldsymbol{v}^{\pm}) = 0$ should be added. It is enough to add the equation for one component, e.g.

$$\nabla(n^+\boldsymbol{v}^+) = 0, \tag{5}$$

because the continuity equation for the second component then follows from (5) and the current continuity equation $\nabla \boldsymbol{j} = 0$ [which, in turn, results from Maxwell's equation $\nabla \times \boldsymbol{B} = (4\,\pi/c)\,\boldsymbol{j}$].

In the limit of infinite particle energy,

$$\gamma = \infty, \quad v_r^{(0)} = c, \quad v_\varphi^{(0)} = 0, \quad v_\theta^{(0)} = 0, \tag{6}$$

so that

$$\rho_\mathrm{e} = \rho_\mathrm{s}\frac{R^2}{r^2}\cos\theta, \quad j_r = \rho_\mathrm{s} c\frac{R^2}{r^2}\cos\theta, \quad j_\theta = j_\varphi = 0, \tag{7}$$

the monopole poloidal magnetic field

$$B_r^{(0)} = B_0\frac{R^2}{r^2}, \quad B_\theta^{(0)} = 0, \tag{8}$$

is an exact solution of Maxwell's equations. In this case,

$$B_\varphi^{(0)} = E_\theta^{(0)} = -B_0\frac{\Omega R}{c}\frac{R}{r}\sin\theta, \tag{9}$$

$$E_r^{(0)} = E_\varphi^{(0)} = 0, \tag{10}$$

which is just the well-known Michel (1973) solution. Here B_0 and ρ_s are the magnetic field and charge density on the surface $r = R \ll R_\mathrm{L}$, and the angular velocity is $\Omega = 2\pi c\,|\rho_\mathrm{s}|/B_0$. The limit $\gamma \to \infty$ corresponds to zero particle mass in the force-free approximation.

It is also convenient to introduce the electric field potential $\Phi(r, \theta)$, so that $\boldsymbol{E} = -\nabla\Phi$ and

$$\Phi^{(0)} = -\frac{\Omega R^2 B_0}{c}\cos\theta \tag{11}$$

and the flux function $\Psi(r, \theta)$, so that the poloidal magnetic field

$$\boldsymbol{B}_\mathrm{p} = \frac{\nabla\Psi \times \boldsymbol{e}_\varphi}{2\pi r\sin\theta} \tag{12}$$

and $\Psi^{(0)} = 2\pi\,B_0\,R^2(1 - \cos\theta)$.

Then the dimensionless corrections $\eta^\pm(r, \theta)$, $\boldsymbol{\xi}^\pm(r, \theta)$, $\delta(r, \theta)$, $\varepsilon\,f(r, \theta)$ and $\zeta(r, \theta)$ for the case $v \neq c$ can be introduced in the following form:

$$n^+ = \frac{\Omega B_0}{2\pi c e}\frac{R^2}{r^2}\left[\lambda - \frac{1}{2}\cos\theta + \eta^+(r, \theta)\right], \tag{13}$$

$$n^- = \frac{\Omega B_0}{2\pi c e}\frac{R^2}{r^2}\left[\lambda + \frac{1}{2}\cos\theta + \eta^-(r, \theta)\right], \tag{14}$$

$$v_r^\pm = c\left[1 - \xi_r^\pm(r, \theta)\right], \qquad v_\theta^\pm = c\xi_\theta^\pm(r, \theta),$$

$$v_\varphi^\pm = c\xi_\varphi^\pm(r, \theta), \tag{15}$$

$$\Phi(r, \theta) = \frac{\Omega R^2 B_0}{c}\left[-\cos\theta + \delta(r, \theta)\right], \tag{16}$$

$$\Psi(r, \theta) = 2\pi B_0 R^2\left[1 - \cos\theta + \varepsilon\,f(r, \theta)\right], \tag{17}$$

and thus

$$B_r = B_0\frac{R^2}{r^2}\left(1 + \frac{\varepsilon}{\sin\theta}\frac{\partial f}{\partial\theta}\right), \tag{18}$$

$$B_\theta = -\varepsilon\frac{B_0 R^2}{r\sin\theta}\frac{\partial f}{\partial r}, \tag{19}$$

$$B_\varphi = B_0\frac{R\Omega}{c}\frac{R}{r}\left[-\sin\theta - \zeta(r, \theta)\right], \tag{20}$$

$$E_r = -\frac{\Omega B_0 R^2}{c}\frac{\partial\delta}{\partial r}, \tag{21}$$

$$E_\theta = \frac{\Omega R^2 B_0}{cr}\left(-\sin\theta - \frac{\partial\delta}{\partial\theta}\right), \tag{22}$$

where $\lambda \gg 1$ is the multiplication parameter ($\lambda = e n_\mathrm{s}/|\rho_\mathrm{s}|$, where n_s is the number density of particles on the surface $r = R$). For $\lambda < 1$ the approach under consideration is not valid. In the following, for simplicity, we consider the case $\lambda =$ constant. Such a choice corresponds to a constant particle-to-magnetic flux ratio $\kappa =$ constant.

Switching to dimensionless variables, below we use the dimensionless radius $x = r/R_\mathrm{L} = r\,\Omega/c$ and the dimensionless drag force:

$$F_\mathrm{d}^\pm = \frac{4}{3}\frac{\sigma_\mathrm{T} U_\mathrm{iso}}{\Omega m_\mathrm{e} c}(\gamma^\pm)^2. \tag{23}$$

Now, substituting (13)–(22) into (3) we obtain, to first order in all the correcting functions, the following system of equations:

$$-\frac{1}{\sin\theta}\frac{\partial}{\partial\theta}(\zeta\sin\theta)=2(\eta^+-\eta^-)-2\left[\left(\lambda-\frac{1}{2}\cos\theta\right)\xi_r^+-\left(\lambda+\frac{1}{2}\cos\theta\right)\xi_r^-\right], \tag{24}$$

$$2(\eta^+-\eta^-)+\frac{\partial}{\partial x}\left(x^2\frac{\partial\delta}{\partial x}\right)+\frac{1}{\sin\theta}\frac{\partial}{\partial\theta}\left(\sin\theta\frac{\partial\delta}{\partial\theta}\right)=0, \tag{25}$$

$$\frac{\partial\zeta}{\partial x}=\frac{2}{x}\left[\left(\lambda-\frac{1}{2}\cos\theta\right)\xi_\theta^+-\left(\lambda+\frac{1}{2}\cos\theta\right)\xi_\theta^-\right], \tag{26}$$

$$-\frac{\varepsilon}{\sin\theta}\frac{\partial^2 f}{\partial x^2}-\frac{\varepsilon}{x^2}\frac{\partial}{\partial\theta}\left(\frac{1}{\sin\theta}\frac{\partial f}{\partial\theta}\right)=\frac{2}{x}\left[\left(\lambda-\frac{1}{2}\cos\theta\right)\xi_\varphi^+-\left(\lambda+\frac{1}{2}\cos\theta\right)\xi_\varphi^-\right], \tag{27}$$

$$\frac{\partial}{\partial x}\left(\xi_\theta^+\gamma^+\right)+\frac{\xi_\theta^+\gamma^+}{x}=-\xi_\theta^+F_{\rm d}^+\left(\frac{m_{\rm e}}{m_{\rm p}}\right)^3+4\lambda\sigma\left(\frac{m_{\rm e}}{m_{\rm p}}\right)\left(-\frac{1}{x}\frac{\partial\delta}{\partial\theta}+\frac{\zeta}{x}-\frac{\sin\theta}{x}\xi_r^++\frac{1}{x^2}\xi_\varphi^+\right), \tag{28}$$

$$\frac{\partial}{\partial x}\left(\xi_\theta^-\gamma^-\right)+\frac{\xi_\theta^-\gamma^-}{x}=-\xi_\theta^-F_{\rm d}^--4\lambda\sigma\left(-\frac{1}{x}\frac{\partial\delta}{\partial\theta}+\frac{\zeta}{x}-\frac{\sin\theta}{x}\xi_r^-+\frac{1}{x^2}\xi_\varphi^-\right), \tag{29}$$

$$\frac{\partial}{\partial x}(\gamma^+)=-F_{\rm d}^+\left(\frac{m_{\rm e}}{m_{\rm p}}\right)^3+4\lambda\sigma\left(\frac{m_{\rm e}}{m_{\rm p}}\right)\left(-\frac{\partial\delta}{\partial x}-\frac{\sin\theta}{x}\xi_\theta^+\right), \tag{30}$$

$$\frac{\partial}{\partial x}(\gamma^-)=-F_{\rm d}^--4\lambda\sigma\left(-\frac{\partial\delta}{\partial x}-\frac{\sin\theta}{x}\xi_\theta^-\right), \tag{31}$$

$$\frac{\partial}{\partial x}\left(\xi_\varphi^+\gamma^+\right)+\frac{\xi_\varphi^+\gamma^+}{x}=-\xi_\varphi^+F_{\rm d}^+\left(\frac{m_{\rm e}}{m_{\rm p}}\right)^3+4\lambda\sigma\left(\frac{m_{\rm e}}{m_{\rm p}}\right)\left(-\varepsilon\frac{1}{x\sin\theta}\frac{\partial f}{\partial x}-\frac{1}{x^2}\xi_\theta^+\right), \tag{32}$$

$$\frac{\partial}{\partial x}\left(\xi_\varphi^-\gamma^-\right)+\frac{\xi_\varphi^-\gamma^-}{x}=-\xi_\varphi^-F_{\rm d}^--4\lambda\sigma\left(-\varepsilon\frac{1}{x\sin\theta}\frac{\partial f}{\partial x}-\frac{1}{x^2}\xi_\theta^-\right), \tag{33}$$

where

$$\sigma=\frac{\Omega eB_0R^2}{4\lambda m_{\rm e}c^3}\gg1 \tag{34}$$

is the Michel (1969) magnetization parameter describing the particle-to-electromagnetic energy flux ratio $W_{\rm part}/W_{\rm em}=(m_{\rm p}/m_{\rm e})\gamma/\sigma$. Hence, for a Poynting-dominated flow we have $\gamma\ll\sigma$. As we see, the disturbances of the particle density η^+ and η^- enter equations (24)–(33) only in the combination $\eta^+-\eta^-$. Therefore, the system (24)–(33) is closed, but the equation of mass continuity (5) is necessary to determine η^+ and η^- separately. The system (24)–(33) differs from that considered by Beskin & Rafikov (2000, hereafter Paper II) only by the additional drag terms in the right-hand side of (28)–(33).

2.2 The one-fluid limit

Equations (24)–(33) describe the flow in the two-fluid approximation. We now reduce the complete system of equations (24)–(33) to consider the one-fluid approximation. In the case of an electron–proton outflow there is a small parameter $m_{\rm e}/m_{\rm p}\sim10^{-3}$, which allows us to neglect the electron mass and thus to proceed in a standard way to the one-fluid approximation. However, as demonstrated in Paper II, this can also be performed in the electron–positron case for a magnetically dominated ($\sigma\gg1$) dense ($\lambda\gg1$) plasma. Because the non-hydrodynamic components of the velocity are small in this case (cf. Melatos & Melrose 1996),

$$\frac{\Delta\xi_r^\pm}{\xi_r}\sim\lambda^{-1}\sigma^{-2/3},\qquad\frac{\Delta\xi_\theta^\pm}{\xi_\theta}\sim\lambda^{-1},\qquad\frac{\Delta\xi_\varphi^\pm}{\xi_\varphi}\sim\lambda^{-1}\sigma^{-2/3}, \tag{35}$$

we can set $\xi_i^+=\xi_i^-=\xi_i$ ($i=r,\theta,\varphi$), where ξ_i is the hydrodynamic velocity. In this limit we also have

$$\frac{\delta-\varepsilon f}{\varepsilon f}\sim\lambda^{-2}\sigma^{-2/3}. \tag{36}$$

As a result, for a magnetically dominated outflow with $\sigma\gg1$ and $\lambda\gg1$ in the one-fluid approximation,

$$\delta=\varepsilon f. \tag{37}$$

Finally, taking equations (28) and (29) together with (37) in the limit $\lambda\sigma\gg1$ into consideration give another useful one-fluid relation:

$$-\varepsilon\frac{1}{x}\frac{\partial f}{\partial\theta}+\frac{\zeta}{x}-\frac{\sin\theta}{x}\xi_r+\frac{1}{x^2}\xi_\varphi=0, \tag{38}$$

this equation being the same as in the drag-free case. On the other hand, as demonstrated in Paper II,

$$\frac{\xi_\theta}{\xi_\varphi}\approx\sigma^{-1/3}. \tag{39}$$

Hence, in the one-fluid approximation one can set $\xi_\theta = 0$ so that

$$\gamma^2 = \frac{1}{2\xi_r - \xi_\varphi^2}. \tag{40}$$

It is necessary to stress that in some cases the monopole geometry allows one to separately consider the set of equations describing the particle energy and the set of equations resulting in the Grad–Shafranov (GS) equation, which determines the disturbance of magnetic surfaces. Thus, here we can consider particle energy without formulating the general form of the GS equation. Some asymptotics of the GS equation are discussed below.

3 THE ELECTRON–POSITRON OUTFLOW

3.1 Integrals of motion

In this section we consider the properties of the electron–positron outflow when $m_\mathrm{p} = m_\mathrm{e} = m$. In our simple geometry with a (split) monopole poloidal magnetic field in the zeroth approximation the particle motion can be considered as radial. It allows us to integrate some equations along the r coordinate axis. This feature was first demonstrated by Li et al. (1992).

Indeed, combining (30) and (31) with (26) one can obtain in the one-fluid approximation

$$\zeta = \frac{l(\theta)}{\sin\theta} + \frac{2\varepsilon}{\tan\theta} f - \frac{1}{\sigma \sin\theta}(\gamma - \gamma_\mathrm{in}) - \frac{1}{\sigma \sin\theta} l_\mathrm{A} \int_{x_0}^{x} u(x')\gamma^2(x')\, \mathrm{d}x', \tag{41}$$

where γ_in is the Lorentz factor near the origin, $x_0 = \Omega R/c$, and the integration constant $l(\theta)$ describes the disturbance of the electric current $I(R,\theta) = I_A[\sin^2\theta + l(\theta)]$ on the surface $r = R$. The integration constant must be determined from the critical conditions on singular surfaces. The compactness parameter l_A is defined by the relation

$$l_\mathrm{A} = \frac{4}{3}\frac{\sigma_\mathrm{T} U_\mathrm{A}}{m_\mathrm{e} c \Omega}, \tag{42}$$

where $U_\mathrm{A} = U(R_\mathrm{L})$ is again the first term in (1) on the light cylinder $r = R_\mathrm{L}$. Finally, we also denote

$$l_\mathrm{ext} = \frac{4}{3}\frac{\sigma_\mathrm{T} U_\mathrm{ext}}{mc\Omega}, \tag{43}$$

so that (1) for $x > 1$ can be rewritten as

$$u(x) = x^{-n} + l_\mathrm{ext}/l_\mathrm{A}. \tag{44}$$

For $x < 1$ it is natural to set $u(x) = 1$.

Expression (41) is just another way of writing the diminishing of the Bernouilli integral E_B along a magnetic field line as a result of the drag force. Within the Grad–Shafranov approach the full energy loss is determined by $W = \int E_B\, \mathrm{d}\Psi$. Thus relation (41) can be rewritten as

$$E_B(r) = E_B(R) - \frac{\lambda\Omega}{2\pi e}\int_R^r F_\mathrm{drag}\, \mathrm{d}r, \tag{45}$$

where the energy flux per unit magnetic flux E_B has the standard form $E_B = \Omega\, I/2\pi\, c + \gamma mc^2\kappa$. Here I is the total electric current inside the magnetic tube and κ is the particle-to-magnetic flux ratio (see, e.g., Beskin 1997 for details).

In the following we consider the case $\gamma_\mathrm{in} \sim 1$, i.e.

$$\gamma_\mathrm{in}^3 \ll \sigma, \tag{46}$$

when additional acceleration of particles inside the fast magnetosonic surface takes place (see, e.g., Paper I). In the case where $\gamma_\mathrm{in}^3 \gg \sigma$ corresponds to ordinary pulsars, the particle energy remains constant ($\gamma = \gamma_\mathrm{in}$) on any way up to the fast magnetosonic surface (Bogovalov 1997).

The other two integrals of motion, namely the conservation of angular momentum separately for electrons and positrons, can be obtained from equations (30)–(33):

$$\gamma^+(1 - x\sin\theta\xi_\varphi^+) = \gamma_\mathrm{in}^+ - l_\mathrm{A}\int_{x_0}^{x} u(x')(1 - x'\sin\theta\xi_\varphi^+)(\gamma^+)^2\, \mathrm{d}x' - 4\lambda\sigma(\delta - \varepsilon f), \tag{47}$$

$$\gamma^-(1 - x\sin\theta\xi_\varphi^-) = \gamma_\mathrm{in}^- - l_\mathrm{A}\int_{x_0}^{x} u(x')(1 - x'\sin\theta\xi_\varphi^-)(\gamma^-)^2\, \mathrm{d}x' + 4\lambda\sigma(\delta - \varepsilon f). \tag{48}$$

In the one-fluid approximation this gives

$$\gamma(1 - x\sin\theta\xi_\varphi) = \gamma_\mathrm{in} - l_\mathrm{A}\int_{x_0}^{x} u(x')(1 - x'\sin\theta\xi_\varphi)\gamma^2(x')\, \mathrm{d}x'. \tag{49}$$

At large distances, where $\gamma \gg \gamma_\mathrm{in}$, we have

$$\xi_\varphi \approx \frac{1}{x\sin\theta}. \tag{50}$$

It can be seen from (49) that the presence of the drag force (the term proportional to l_A) makes this approximation more accurate.

3.2 Fast magnetosonic surface

Substituting ζ from (41), ξ_r from (40), and ξ_φ from (49) into (38) we obtain the following equation to determine the position of the fast magnetosonic surface $r = r_{\rm F}$:

$$-\varepsilon\frac{\partial f}{\partial\theta}+\frac{2\varepsilon}{\tan\theta}f+\frac{l(\theta)}{\sin\theta}-\frac{1}{\sigma\sin\theta}(\gamma-\gamma_{\rm in}+J)-\sin\theta\left[\frac{1}{2\gamma^2}+\frac{(\gamma-\gamma_{\rm in}+J_1)^2}{2x^2\gamma^2\sin^2\theta}\right]+\frac{\gamma-\gamma_{\rm in}+J_1}{x^2\gamma\sin\theta}=0, \tag{51}$$

where

$$J=l_{\rm A}\int_{x_0}^{x}u(x')\gamma^2(x')\,{\rm d}x', \tag{52}$$

$$J_1=l_{\rm A}\int_{x_0}^{x}u(x')\gamma^2(x')(1-x'\sin\theta\xi_\varphi)\,{\rm d}x'. \tag{53}$$

However, in accordance with (49) and thereafter, the terms J_1 and $\gamma_{\rm in}$ can be neglected far from the origin of the flow $r \gg R_{\rm L}$. Also, since $l(\theta)\sim\sigma^{-4/3}$ (see Paper I), the term with $l(\theta)$ can also be omitted. Hence, one can write down the following algebraic equation for the Lorentz factor γ:

$$\gamma^3-\sigma\left(P+\frac{1}{2x^2}\right)\gamma^2+\frac{1}{2}\sigma\sin^2\theta=0, \tag{54}$$

where

$$P=-\frac{J}{\sigma}+2\varepsilon f\cos\theta-\varepsilon\sin\theta\frac{\partial f}{\partial\theta}. \tag{55}$$

This differs from the drag-free case by the additional term J/σ.

Equation (54) allows us to determine the position of the fast magnetosonic surface $r = r_{\rm F}$ and the energy of particles on this surface $\gamma_{\rm F} = \gamma(r_{\rm F})$. Indeed, as the fast magnetosonic surface is the X-point, we find the exact solution for coinciding roots

$$\gamma_{\rm F}=\sigma^{1/3}\sin^{2/3}\theta, \tag{56}$$

which does not depend on P at all, or thus on the drag force. On the other hand, both the numerator and the denominator of the derivative ${\rm d}\gamma/{\rm d}x$ must be equal to zero on the surface $r = r_{\rm F}$:

$$x\frac{{\rm d}\gamma}{{\rm d}x}=\frac{\gamma\sigma(x{\rm d}P/{\rm d}x-x^{-2})}{3\gamma-\sigma(2P+x^{-2})}. \tag{57}$$

It gives

$$(P+x^{-2})_{\rm F}\approx\sigma^{-2/3},\qquad |P|_{\rm F}\approx|x^{-2}|_{\rm F}. \tag{58}$$

Now using (55), one can see that the conditions for weak and strong drag are, respectively, $l_{\rm A}\ll l_{\rm cr}$ and $l_{\rm A}\gg l_{\rm cr}$, where

$$l_{\rm cr}=\sigma^{1/3}. \tag{59}$$

In other words, for $l_{\rm A}\ll l_{\rm cr}$ the flow remains the same as in the drag-free case, and

$$x_{\rm F}\approx\sigma^{1/3}\sin^{-1/3}\theta, \tag{60}$$

$$(\varepsilon f)_{\rm F}\approx\sigma^{-2/3}. \tag{61}$$

On the other hand, for a high enough photon density $l_{\rm A}\gg l_{\rm cr}$ one can obtain, for $n = 3$,

$$x_{\rm F}\approx\left(\frac{\sigma}{l_{\rm A}}\right)^{1/2}=\sigma^{1/3}\left(\frac{l_{\rm cr}}{l_{\rm A}}\right)^{1/2}, \tag{62}$$

$$(\varepsilon f)_{\rm F}\approx\frac{l_{\rm A}}{\sigma}. \tag{63}$$

Thus, as we can see, the energy $\gamma_{\rm F}mc^2$ does not depend on the drag. The disturbance of the magnetic surfaces increases with increasing $l_{\rm A}$, but remains small for $l_{\rm A}\ll\sigma$.

For a very dense photon field, according to (41) and (63), the disturbance of the magnetic surfaces becomes of the order of unity for $l_{\rm A}\sim l_{\rm max}$ where

$$l_{\rm max}=\sigma, \tag{64}$$

i.e. when the disturbance of the Bernouilli integral $\Delta E_B = E_B(r) - E_B(R_{\rm L})$ (45) is of the order of the total energy flux E_B, or in other words when the drag force substantially diminishes the total energy flux of the flow. However, this means that the disturbance of the magnetic surfaces becomes large when the energies of particles in the vicinity of the fast magnetosonic surface become non-relativistic. This feature is well known for a drag-free flow both within numerical (Sakurai 1985; Bogovalov 1997) and analytical (Bogovalov 1992; Tomimatsu 1994; Paper I) considerations. Of course, our analysis within the small disturbance approach can only demonstrate the tendency. For this reason, within our approach σ = constant. In reality, since $\sigma = E_B/(mc^2\kappa)$, a decrease of the energy flux also results in a decrease of σ.

Finally, it is necessary to stress that the results depend significantly on the assumed model of the isotropic photon density. In particular, for the general power-law dependence of the photon density for $n < 3$ in (44), one can obtain for the position of the fast magnetosonic point and the disturbance of the magnetic surfaces

$$x_{\rm F} \approx \sigma^{1/3} \left(\frac{l_{\rm cr}}{l_{\rm A}}\right)^{1/(5-n)}, \tag{65}$$

$$(\varepsilon f)_{\rm F} \approx \left(\frac{l_{\rm A}}{\sigma}\right)^{2/(5-n)} \tag{66}$$

instead of (62) and (63). This takes place for $l_{\rm A} > l_{\rm cr}$, where $l_{\rm cr}$ is the photon density capable of disturbing the magnetically dominated outflow:

$$l_{\rm cr} = \sigma^{(n-2)/3}. \tag{67}$$

A large disturbance $(\varepsilon f)_{\rm F} \sim 1$ can only be realized for a very high photon density $l_{\rm A} > l_{\rm max}$, where again

$$l_{\rm max} = \sigma. \tag{68}$$

For $n \geqslant 3$ [when the value J defined by (52) is determined by the lower limit of integration and does not depend on n] we have $(\varepsilon f)_{\rm F} \approx l_{\rm A}/\sigma$, $x_{\rm F} \approx (\sigma/l_{\rm A})^{1/2}$, $l_{\rm cr} = \sigma^{1/3}$, and $l_{\rm max} = \sigma$, i.e. the same as for $n = 3$. According to (41), $(\varepsilon f)_{\rm F} \sim 1$ occurs when $\Delta E_B/E_B \sim 1$ for all values of n.

3.3 The structure of the flow at small and large distances

3.3.1 Inner region

First, we consider the structure of the flow well within the fast magnetosonic surface $r \ll r_{\rm F}$. As one can see from (54), for $r \ll r_{\rm F}$

$$\gamma \approx \frac{\sin\theta}{(2P + 1/x^2)^{1/2}}. \tag{69}$$

In particular, for $l_{\rm A} \ll l_{\rm cr}$ one can neglect the term P in the denominator. On the other hand, for $l_{\rm A} \gg l_{\rm cr}$ in the immediate vicinity of the fast magnetosonic surface the negative term $-J/\sigma$ in P should to be taken into consideration. As a result, the particle energy increases abruptly up to the value $\sim \sigma^{1/3}$. Nevertheless, for $r \ll r_{\rm F}$ the value P can be omitted for the arbitrary compactness parameter $l_{\rm A}$. It also means that for $r \ll r_{\rm F}$ it is possible to neglect the first two terms in (38). Thus, in the internal region $r \ll r_{\rm F}$ we have

$$\xi_r = \frac{\xi_\varphi}{x\sin\theta}. \tag{70}$$

Now, using relations (50) and (70), one can obtain

$$\gamma^2 = \gamma_{\rm in}^2 + x^2\sin^2\theta \approx x^2\sin^2\theta, \tag{71}$$

$$\xi_\varphi = \frac{\sqrt{\gamma_{\rm in}^2 + x^2\sin^2\theta} - \gamma_{\rm in}}{x\sin\theta\sqrt{\gamma_{\rm in}^2 + x^2\sin^2\theta}} \approx \frac{1}{x\sin\theta}, \tag{72}$$

$$\xi_r = \frac{\sqrt{\gamma_{\rm in}^2 + x^2\sin^2\theta} - \gamma_{\rm in}}{x^2\sin^2\theta\sqrt{\gamma_{\rm in}^2 + x^2\sin^2\theta}} \approx \frac{1}{x^2\sin^2\theta}, \tag{73}$$

in full agreement with the ideal MHD approximation. Hence, one can conclude that: in the internal region $r < r_{\rm F}$ the radiation drag does not affect the particle motion. Here the universal value of the Lorentz factor (71) corresponds to the drift velocity, and it depends on no external disturbances. Indeed, using the frozen-in condition $\boldsymbol{E} + \boldsymbol{v} \times \boldsymbol{B}/c = 0$, we obtain for the drift velocity

$$U_{\rm dr}^2 = c^2\frac{\boldsymbol{E}^2}{\boldsymbol{B}^2} = c^2\left(\frac{B_\varphi^2}{E^2} + \frac{B_r^2}{E^2}\right)^{-1}. \tag{74}$$

In our case, however, according to (16)–(22), we have

$$B_\varphi^2 \approx E^2, \qquad B_r^2 \approx E^2/(x^2\sin^2\theta). \tag{75}$$

These relations immediately lead to the previously stated asymptotic behaviour (71). In particular, this means that disturbance of the magnetic surfaces plays no role in the determination of the particle energy. For this reason, it is possible not to consider the radiation drag corrections to the field structure for $r \ll r_{\rm F}$.

3.3.2 Outer region

In the other limit, well outside the fast magnetosonic surface ($r \gg r_{\rm F}$) equations (41), (38), (24)–(25) and (40) can be rewritten in the form

$$\zeta = \varepsilon\frac{2}{\tan\theta}f - \frac{1}{\sigma\sin\theta}\gamma - \frac{1}{\sigma\sin\theta}l_{\rm A}\int_{x_0}^{x} u(x')\gamma^2(x')\,{\rm d}x', \tag{76}$$

$$\zeta = \varepsilon \frac{\partial f}{\partial \theta} + \sin\theta \xi_r, \tag{77}$$

$$\varepsilon \frac{\partial}{\partial x}\left(x^2 \frac{\partial f}{\partial x}\right) - \frac{1}{\sin^3\theta}\frac{\partial}{\partial \theta}\left(\sin^4\theta \xi_r\right) = 0, \tag{78}$$

$$\gamma^2 = \frac{1}{2\xi_r}, \tag{79}$$

where we neglect the small values $l(\theta)$, $\gamma_{\rm in}/\gamma$ and ξ_φ, and set $\delta = \varepsilon f$. As we can see, the only correction compared with the drag-free case is the last additional term in (76). Without the drag force the system (76)–(79) results in a very slow increase in the particle energy ($\gamma \propto \ln^{1/3} r$) and actually in the absence of collimation, $\varepsilon f \sim \sigma^{-2/3} \ln^{1/3} r$ (Tomimatsu 1994; Paper I). Unfortunately, because of the non-linearity of the system (76)–(79), in the general case it is impossible to reduce it to the GS equation for the magnetic disturbance εf only. For this reason, in the following we only present an asymptotic representation of the GS equation.

(i) Low photon density $l_{\rm A} \ll l_{\rm cr}$.

In this case the action of drag results in a small correction to the particle energy. Only at very large distances, where the first term in (44) can be neglected, does the drag significantly change the energy of particles. Indeed, for the decreasing component of the isotropic photon density [$u(x) \sim x^{-n}$ in 44] and for an almost constant particle energy the drag term in (76) does not increase with the distance r. Here increasing the drag term is due to the homogeneous part of the photon density ($l_{\rm ext}/l_{\rm A}$ in 44). Clearly, this can be realized at large enough distances [$r > R_{\rm L}(l_{\rm A}/l_{\rm ext})\sigma^{(3-n)/3}$], where the contribution from external photons is the leading one. Thus, we see that the action of the drag force can be significant for a high enough density of external isotropic photons in the vicinity of the compact object.

Now we consider this asymptotic region in more detail. Neglecting the term containing γ in (76) and the first term in (44), one can obtain for the generalized GS equation

$$\varepsilon \frac{\partial}{\partial x}\left(x^2 \frac{\partial f}{\partial x}\right) - \frac{1}{\sin^3\theta}\frac{\partial}{\partial \theta}\left[2\varepsilon \sin^2\theta \cos\theta f - \varepsilon \sin^3\theta \frac{\partial f}{\partial \theta} - \frac{\sin^2\theta}{\sigma} l_{\rm ext} \int_{x_0}^{x} \gamma^2(x')\, {\rm d}x'\right] = 0. \tag{80}$$

One can seek the solution of this equation in the form

$$\varepsilon f(x,\theta) \propto x^{\alpha_\delta}, \qquad \gamma(x,\theta) \propto x^{\alpha_\gamma}. \tag{81}$$

Substituting these expressions into (80) we obtain

$$\varepsilon f(x,\theta) = k_1(\theta) l_{\rm ext}^{1/2} \sigma^{-1/2} x^{1/2}, \tag{82}$$

$$\gamma(x,\theta) = k_2(\theta) l_{\rm ext}^{-1/4} \sigma^{1/4} x^{-1/4}, \tag{83}$$

where $k_1(\theta) \sim k_2(\theta) \sim 1$ describe the θ dependence. This takes place for $r > r_{\rm h}$, where

$$r_{\rm h} = R_{\rm L} l_{\rm ext}^{-1} \sigma^{-1/3}. \tag{84}$$

For $r_{\rm F} < r < r_{\rm h}$ the action of drag is negligible.

As we see, for $r > r_{\rm h}$ the drag force results in a decrease of the particle energy and an additional collimation of the magnetic surfaces outside the fast magnetosonic surface. These asymptotic solutions, however, do not seem to be realized in reality. Indeed, as one can check, $r_{\rm h} \sim (10^6$–$10^8) R_{\rm L} > r_{\rm cloud}$. However, for $r > r_{\rm cloud}$ the model that we adopted for the homogeneous component of the photon density is no longer valid and thus the asymptotic solutions (82) and (83) do not apply. This conclusion is made under the assumption that the homogeneous component is produced by the reradiating clouds surrounding the central engine. One could imagine producing a homogeneous component of the photon density in the host galaxy. However, in this case the photon density $U_{\rm ext}$ is too low and thus the collimation distance $r_{\rm h}$ is too large for our approach to be valid in the region $r \sim r_{\rm h}$.

The characteristic radial dependence of the particle energy in the presence of the drag is demonstrated in Fig. 1(a). One can conclude that for a low photon density: the action of the drag force is very weak unless photon field is present out to distances $r \sim r_{\rm h}$. In the latter case the drag force efficiently reduces the particle energy beyond $r \sim r_{\rm h}$.

It is necessary to stress here an important property of the fast magnetosonic surface for $l_{\rm A} < l_{\rm cr}$. Introducing a small disturbance of the particle energy resulting from the drag

$$\gamma = \gamma_0 + \Delta\gamma, \tag{85}$$

where γ_0 is the Lorentz factor of particles without the drag force, one can obtain from (76)–(79)

$$-\sin^2\theta \frac{\Delta\gamma}{\gamma_0^3} + \varepsilon \frac{\partial \Delta f}{\partial \theta} - 2\varepsilon \cos\theta \Delta f + \frac{1}{\sigma}\Delta\gamma = \frac{J}{\sigma}. \tag{86}$$

As equation (78) results in $\varepsilon \Delta f \sim \Delta\gamma/\gamma_0^3$, we see that outside the fast magnetosonic surface (where $\gamma_0 > \sigma^{1/3}$)

$$mc^2 \Delta\gamma \approx -\int F_{\rm drag}\, {\rm d}r. \tag{87}$$

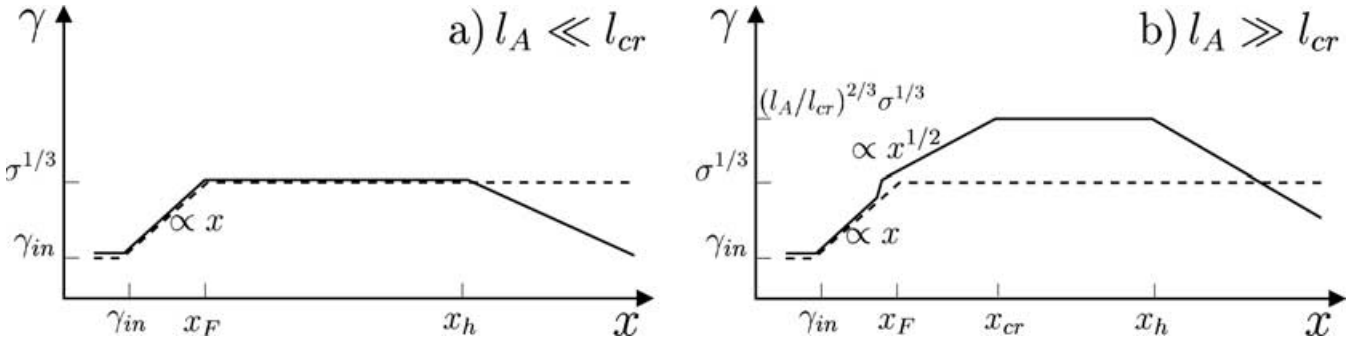

Figure 1. The radial dependence of the Lorentz factor $\gamma(r)$ for low (a) and high (b) photon densities for $n = 3$. The dashed lines correspond to the drag-free case.

On the other hand, within the fast magnetosonic surface we have

$$mc^2|\Delta\gamma| \ll \int F_{\rm drag}\ {\rm d}r, \tag{88}$$

in full agreement with (71). This means that inside the fast magnetosonic surface decreasing the total energy flux E_B results from decreasing the electromagnetic energy flux rather than the particle flux. Outside the fast surface the photons act upon the particle directly. In other words, for $l_{\rm A} < l_{\rm cr}$ the fast magnetosonic surface separates the regions in space where particles are strongly or weakly frozen into the electromagnetic field.

(ii) High photon density $l_{\rm A} > l_{\rm cr}$.

For a high photon density $l_{\rm A} > l_{\rm cr}$ the drag force significantly changes the energy of the outgoing particles. As shown in Fig. 1(b), increasing the particle energy continues outside the fast magnetosonic surface up to the maximum value

$$\gamma_{\rm max} \approx \left(\frac{l_{\rm A}}{l_{\rm cr}}\right)^{4(n-2)/(5n-n^2)} \sigma^{1/3}. \tag{89}$$

For $n < 2$ there is no additional acceleration. Only at larger distances ($r > r_{\rm cr}$) does the radial dependence of the energy of the outgoing plasma become similar to the previous case.

Indeed, outside the fast magnetosonic surface one can neglect the term $\sin\theta\xi_r$ in (77). As a result, the system (76)–(79) can be rewritten in the form

$$\varepsilon\frac{\partial f}{\partial\theta} - \varepsilon\frac{2}{\tan\theta}f = -\frac{1}{\sigma\sin\theta}\gamma - \frac{1}{\sigma\sin\theta}l_{\rm A}\int_{x_0}^{x} u(x')\gamma^2(x')\ {\rm d}x', \tag{90}$$

$$\varepsilon\frac{\partial}{\partial x}\left(x^2\frac{\partial f}{\partial x}\right) - \frac{1}{2\sin^3\theta}\frac{\partial}{\partial\theta}\left(\frac{\sin^4\theta}{\gamma^2}\right) = 0, \tag{91}$$

which results in

$$\frac{\partial}{\partial x}\left(x^2\frac{\partial\gamma}{\partial x}\right) + l_{\rm A}\frac{\partial}{\partial x}\left(x^{2-n}\gamma^2\right) = \frac{\sigma}{2\sin^3\theta}\left[2\cos\theta\frac{\partial}{\partial\theta}\left(\frac{\sin^4\theta}{\gamma^2}\right) - \sin\theta\frac{\partial^2}{\partial\theta^2}\left(\frac{\sin^4\theta}{\gamma^2}\right)\right]. \tag{92}$$

For $l_{\rm A} > l_{\rm cr}$ the Lorentz factor γ increases with x, and the right-hand side in (92) can be omitted. This gives

$$x^2\frac{\partial\gamma}{\partial x} + l_{\rm A}x^{2-n}\gamma^2 = C(\theta), \tag{93}$$

where the integration constant $C(\theta) \approx l_{\rm A}x_{\rm F}^{2-n}\gamma_{\rm F}^2$ for $l_{\rm A} \gg l_{\rm cr}$ actually does not depend on the boundary conditions ${\rm d}\gamma/{\rm d}x$ at $x = x_{\rm F}$. In the following we do not consider the θ dependence.

Now analysing equation (93), one can find that for $x_{\rm F} \ll x \ll x_{\rm cr}$, where

$$x_{\rm cr} \approx \left(\frac{l_{\rm A}}{l_{\rm cr}}\right)^{8/(5n-n^2)} x_{\rm F}, \tag{94}$$

the particle energy increases as

$$\gamma(x) \approx \sigma^{1/3}\left(\frac{x}{x_{\rm F}}\right)^{(n-2)/2} \tag{95}$$

for arbitrary n. As to the disturbance of magnetic surfaces εf, it remains approximately constant: $\varepsilon f \approx (l_{\rm A}/\sigma)^{2/(5-n)}$.

On the other hand, in the saturation region $x \gg x_{\rm cr}$, where one can now neglect the term $l_{\rm A}x^{2-n}\gamma^2$ in (93), we have

$$\gamma(x) = C\left(\frac{1}{x_{\rm b}} - \frac{1}{x}\right), \tag{96}$$

where $x_{\rm b} \approx x_{\rm cr}$. One can easily check that the maximum energy $\gamma_{\rm max} \approx C/x_{\rm cr} \approx \sigma^{1/3}(x_{\rm cr}/x_{\rm F})^{(n-2)/2}$ corresponds to (89). As demonstrated in Fig. 2, the analytical estimate (89) is in good agreement with the numerical integration of equation (93).

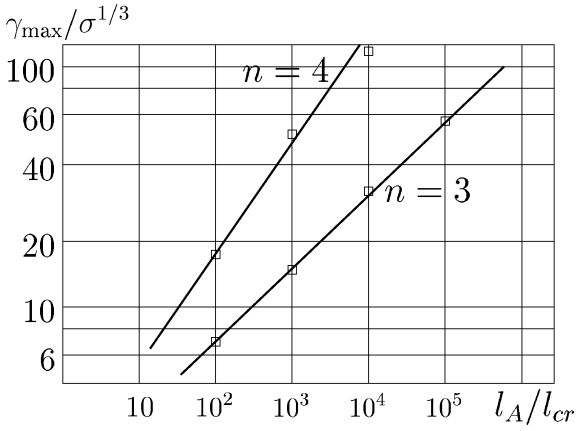

Figure 2. Saturation energy $\gamma_{\max} mc^2$ determined by a numerical integration of (93) for $n = 3$ and 4 (points). The lines correspond to the analytical estimate (89). For $l_A = l_{\max}$, $n \geqslant 3$ we have $\gamma_{\sup} = \sigma^{7/9}$.

3.3.3 Physical interpretation of particle acceleration

At first glance, it is quite unexpected that a drag force can result in an acceleration of particles (so even the word 'drag' itself is not appropriate any more). As was demonstrated, additional acceleration can be realized for a highly magnetized outflow when the photon density decreases rapidly with radius ($n > 2$). This acceleration occurs as a result of the action of the drag force on to magnetic surfaces. Thus, acceleration is only obtained when the disturbance of the magnetic surfaces is taken into account self-consistently.

To understand the nature of the additional particle acceleration in the supersonic region $r > r_{\rm F}$, it is necessary to return to the system (90) and (91). As one can see, equation (91) actually plays the role of the GS equation, describing the force balance in the direction perpendicular to the magnetic surfaces. It contains no drag term, because the drag force acts along the magnetic surfaces. Indeed, as was shown before (Bogovalov 1998; Okamoto 1999; Beskin & Okamoto 2000), in the asymptotic region $r \gg r_{\rm F}$ the transfield GS equation can be written down as $\mathcal{F}_{\rm c} = \mathcal{F}_{\rm em}$, i.e. as a competition between the centrifugal volume force

$$\mathcal{F}_{\rm c} = \frac{nmc^2\gamma + S/c}{R_{\rm c}} \tag{97}$$

and the electromagnetic volume force

$$\mathcal{F}_{\rm em} = \rho_{\rm e} E_\theta + \frac{1}{c} j_\parallel B_\varphi \approx \frac{1}{8\pi r \sin^2\theta} \frac{\partial}{\partial\theta} \left[\left(B_\varphi^2 - E_\theta^2 \right) \sin^2\theta \right], \tag{98}$$

where $S \approx (c/4\pi) E_\theta B_\varphi$ is the Poynting flux. Now using the expression for the curvature radius $R_{\rm c}$ (Begelman & Li 1994; Beskin & Okamoto 2000),

$$\frac{1}{R_{\rm c}} = \frac{\varepsilon}{r \sin\theta} \frac{\partial}{\partial r} \left(r^2 \frac{\partial f}{\partial r} \right) \tag{99}$$

and the condition

$$B_\varphi^2 - E_\theta^2 \approx \frac{1}{\gamma^2} B_\varphi^2 \tag{100}$$

resulting from the relativistic Bernouilli equation (see, e.g., Bogovalov 1998), for a magnetically dominated flow $S \gg nmc^3\gamma$ we recover relation (91).

On the other hand, the Bernouilli equation (90) describes the change of the total energy flux (45) due to the drag force. As was shown above, for $l_{\rm A} > l_{\rm cr}$ in the vicinity of the fast magnetosonic surface the leading terms in the energy equation (90) are those containing εf and $l_{\rm A}$. This means that here the drag force again acts mainly on the electromagnetic (Poynting) flux S. The drag diminishes the θ-component of the electric field E_θ, i.e. it disturbs the equipotential surfaces $\delta(r, \theta)$ =constant. However, since in the one-fluid approximation the magnetic surfaces $\varepsilon f(r, \theta) =$ constant must follow the equipotential surfaces, decreasing the electric field E_θ also results in a change of the curvature of magnetic field lines. As the condition $\mathcal{F}_{\rm c} = \mathcal{F}_{\rm em}$ can now be rewritten in the form

$$\gamma^2 \approx \frac{4\pi j_\parallel}{cE_\theta} R_{\rm c} \approx \frac{R_{\rm c}}{r}, \tag{101}$$

we see that increasing the curvature radius $R_{\rm c}$ faster than r results in an increase in the particle energy. In our case such an acceleration is due to the rapid decrease ($n > 2$) of the isotropic photon density with the distance r.

Thus, we see that for high enough photon density there is an additional acceleration of outgoing plasma outside the fast magnetosonic surface. On the other hand, as for $l_{\rm A} > l_{\max}$ (64) the drag force significantly diminishes the total energy flux E, one can conclude that this

acceleration may only take place up to the energy

$$\mathcal{E}_{\rm sup} \sim \sigma^{1/3} \left(\frac{l_{\rm max}}{l_{\rm cr}}\right)^{4(n-2)/n(5-n)} m_{\rm e}c^2 \tag{102}$$

for $2 < n < 3$. On the other hand, $\mathcal{E}_{\rm sup} \sim \sigma^{7/9} m_{\rm e}c^2$ for $n \geqslant 3$. This energy is always much lower than $\sigma m_{\rm e}c^2$, corresponding to the total conversion of electromagnetic energy into particle energy.

4 THE ELECTRON–PROTON OUTFLOW

In this section we briefly consider the results of the analysis of the electron–proton outflow. As the procedure is quite similar to the electron–positron case, here we present the principal relations only.

The main difference from the electron–positron case, which occurs due to the large mass ratio, is that the drag force acts on the electron component only, and the mass flow is determined entirely by protons. As a result, the energy conservation law has the form

$$\begin{aligned}\zeta &= \frac{2\varepsilon}{\tan\theta} f - \frac{(\lambda + \cos\theta/2)\gamma^- + (m_{\rm p}/m_{\rm e})(\lambda - \cos\theta/2)\gamma^+}{2\lambda\sigma\sin\theta} \\ &\quad - \frac{l_{\rm A}}{2\lambda\sigma\sin\theta}\int_{x_0}^{x}\left[\left(\lambda + \frac{1}{2}\cos\theta\right)(\gamma^-)^2 + \left(\frac{m_{\rm e}}{m_{\rm p}}\right)^2\left(\lambda + \frac{1}{2}\cos\theta\right)(\gamma^+)^2\right] u(x')\gamma^2(x')\,{\rm d}x' \\ &\approx \frac{2\varepsilon}{\tan\theta} f - \left(\frac{m_{\rm p}}{m_{\rm e}}\right)\frac{\gamma}{2\sigma\sin\theta} - \frac{1}{2\sigma\sin\theta} l_{\rm A}\int_{x_0}^{x} u(x')\gamma^2(x')\,{\rm d}x',\end{aligned} \tag{103}$$

where now $\gamma = \gamma^+$. The conservation of angular momentum (47) and (48) looks like

$$\gamma^+(1 - x\sin\theta\xi_\varphi^+) = \gamma_{\rm in}^+ - l_{\rm A}\left(\frac{m_{\rm e}}{m_{\rm p}}\right)^3\int_{x_0}^{x} u(x')(1 - x'\sin\theta\xi_\varphi^+)(\gamma^+)^2\,{\rm d}x' - 4\lambda\sigma\frac{m_{\rm e}}{m_{\rm p}}(\delta - \varepsilon f), \tag{104}$$

$$\gamma^-(1 - x\sin\theta\xi_\varphi^-) = \gamma_{\rm in}^- - l_{\rm A}\int_{x_0}^{x} u(x')(1 - x'\sin\theta\xi_\varphi^-)(\gamma^-)^2{\rm d}x' + 4\lambda\sigma(\delta - \varepsilon f), \tag{105}$$

resulting in $\xi_\varphi = 1/x\sin\theta$. Since for $r \ll r_{\rm F}$ we again have $\xi_r = \xi_\varphi/(x\sin\theta)$, we return to the universal dependence

$$\gamma \approx x\sin\theta. \tag{106}$$

Equation (54) determining the energy on the fast magnetosonic surface now has the form

$$\gamma^3 - 2\sigma\frac{m_{\rm e}}{m_{\rm p}}\left[2\varepsilon f\cos\theta - \varepsilon\sin\theta\frac{\partial f}{\partial\theta} - \frac{1}{2}\frac{l_{\rm A}}{\sigma}\int_{x_0}^{x} u(x')\gamma^2(x')\,{\rm d}x' + \frac{1}{2x^2}\right]\gamma^2 + \frac{m_{\rm e}}{m_{\rm p}}\sigma\sin^2\theta = 0. \tag{107}$$

Hence, for arbitrary $l_{\rm A}$ the Lorentz factor of particles can be presented in the form

$$\gamma_{\rm F} = \left(\frac{2m_{\rm e}}{m_{\rm p}}\right)^{1/3}\sigma^{1/3}\sin^{2/3}\theta. \tag{108}$$

Now, for $l_{\rm A} < l_{\rm cr}^{\rm (p)}$ the position of the fast magnetosonic surface and the disturbance of magnetic surfaces on the fast magnetosonic surface are

$$x_{\rm F} \approx \left(\frac{2m_{\rm e}}{m_{\rm p}}\right)^{1/3}\sigma^{1/3}\sin^{-1/3}\theta, \tag{109}$$

$$(\varepsilon f)_{\rm F} \approx \left(\frac{2m_{\rm e}}{m_{\rm p}}\right)^{-2/3}\sigma^{-2/3}, \tag{110}$$

where for $n < 3$ we have

$$l_{\rm cr}^{\rm (p)} = \left(\frac{m_{\rm p}}{m_{\rm e}}\right)^{(5-n)/3}\sigma^{(n-2)/3} \tag{111}$$

and for $n \geqslant 3$ we have $l_{\rm cr}^{\rm (p)} = (m_{\rm p}/m_{\rm e})^{2/3}\sigma^{1/3}$. On the other hand, for $l_{\rm A} > l_{\rm cr}^{\rm (p)}$ we return to the relations $x_{\rm F} = (\sigma/l_{\rm A})^{1/2}$, $(\varepsilon f)_{\rm F} = l_{\rm A}/\sigma$ for $n \geqslant 3$, but for $n < 3$ now

$$x_{\rm F} \approx \left(\frac{\sigma}{l_{\rm A}}\right)^{1/(5-n)}, \tag{112}$$

$$(\varepsilon f)_{\rm F} \approx \left(\frac{l_{\rm A}}{\sigma}\right)^{2/(5-n)}. \tag{113}$$

As we see, for the disturbance of magnetic surfaces and the position of the fast magnetosonic surface remain the same as for the electron–positron outflow. In particular, the terminating compactness parameter $l_{\rm max} = \sigma$ is again determined by electrons.

Thus, one can conclude that inside the fast magnetosonic surface $r < r_{\rm F}$ the Lorentz factors of all particles are given by the universal relation (106). Hence, our results demonstrate that the drag force does not affect the structure of the flow inside the fast magnetosonic surface for both the electron–positron and the electron–proton cases. However, the position of the fast magnetosonic surface and the critical value of the photon density depend on the mass of the outgoing particles, and for the electron–proton case they are determined by protons.

At large distances $r > r_{\rm F}$ for $l_{\rm A} < l_{\rm cr}^{(\rm p)}$ the particle energy actually remains the same as on the fast magnetosonic surface [$\gamma(r > r_{\rm F}) \approx \gamma_{\rm F}$], while for $l_{\rm A} > l_{\rm cr}^{(\rm p)}$ the Lorentz factor increases up to the maximum value

$$\gamma_{\max} \approx \gamma_{\rm F} \left[\frac{l_{\rm A}}{l_{\rm cr}^{(\rm p)}}\right]^{4(n-2)/(5n-n^2)} \tag{114}$$

for $n < 3$. This takes place up to the distance $r \approx r_{\rm cr}$, where

$$r_{\rm cr} = r_{\rm F} \left[\frac{l_{\rm A}}{l_{\rm cr}^{(\rm p)}}\right]^{8/(5n-n^2)}. \tag{115}$$

Clearly, this additional acceleration can only be realized for $\sigma > m_{\rm p}/m_{\rm e}$. Then, for $n = 3$ we have

$$\mathcal{E}_{\rm sup} \sim \left(\frac{m_{\rm p}}{m_{\rm e}}\right)^{2/9} \sigma^{7/9} m_{\rm e} c^2. \tag{116}$$

5 DISCUSSION AND ASTROPHYSICAL APPLICATIONS

We have demonstrated how for a simple geometry it is possible to determine a small radiation-drag-force correction to the one-fluid ideal MHD outflow. The disturbance of magnetic surfaces was self-consistently taken into consideration. As a result, it is possible to characterize the general influence of the drag action on the magnetic field structure for an ideal magnetically dominated quasi-monopole cold outflow and to determine under what circumstances radiation drag is important.

As demonstrated above, the characteristics of the flow are determined by two main parameters, namely the compactness parameter $l_{\rm A}$ (42) (which is proportional to the photon density) and the magnetization parameter σ (34). If the photon density is low, so that the compactness parameter is small $l_{\rm A} \ll l_{\rm cr}(\sigma)$, the action of the drag force is negligible, while for a high photon density $l_{\rm A} \gg l_{\rm cr}(\sigma)$, particles are additionally accelerated outside the fast magnetosonic surface.

In particular, for $l_{\rm cr} \ll l_{\rm A} \ll l_{\max}$ increasing the drag force results in an increase in the outgoing plasma energy $\mathcal{E}_{\max} \approx \gamma_{\max} m_{\rm e,p} c^2$, but the disturbance of magnetic surfaces is small ($\varepsilon f \ll 1$). For $l_{\rm A} \sim l_{\max}$ an increase in the photon density results in increasing collimation up to values $\varepsilon f \sim 1$, but the particle energy remains near the saturation value $\mathcal{E}_{\rm sup}$. Finally, for a very high photon density $l_{\rm A} \gg l_{\max}$ an effective collimation of magnetic surfaces becomes possible, but in this case the drag force substantially diminishes the flux of electromagnetic energy inside the fast magnetosonic surface. As a result, for $l_{\rm A} \gg l_{\max}$ almost all the energy of the electromagnetic field is lost via the inverse Compton interaction of particles with external photons. For this reason, the very existence of a magnetically dominated flow becomes impossible. The dependence of the maximum particle energy $\mathcal{E}_{\max} = \gamma_{\max} m_{\rm e,p} c^2$ on the compactness parameter $l_{\rm A}$ is shown in Fig. 3.

We now consider several astrophysical applications.

5.1 Active galactic nuclei

For AGN (the central engine is assumed to be a rotating black hole with mass $M \sim 10^9$ $\rm M_\odot$, $R \sim 10^{14}$ cm, the total luminosity $L \sim 10^{45}$ erg s^{-1}, $B_0 \sim 10^4$ G) the compactness parameter $l_{\rm A}$ (42) can be evaluated as

$$l_{\rm A} \approx 30 M_9^{-1} \left(\frac{\Omega R}{c}\right) L_{45}. \tag{117}$$

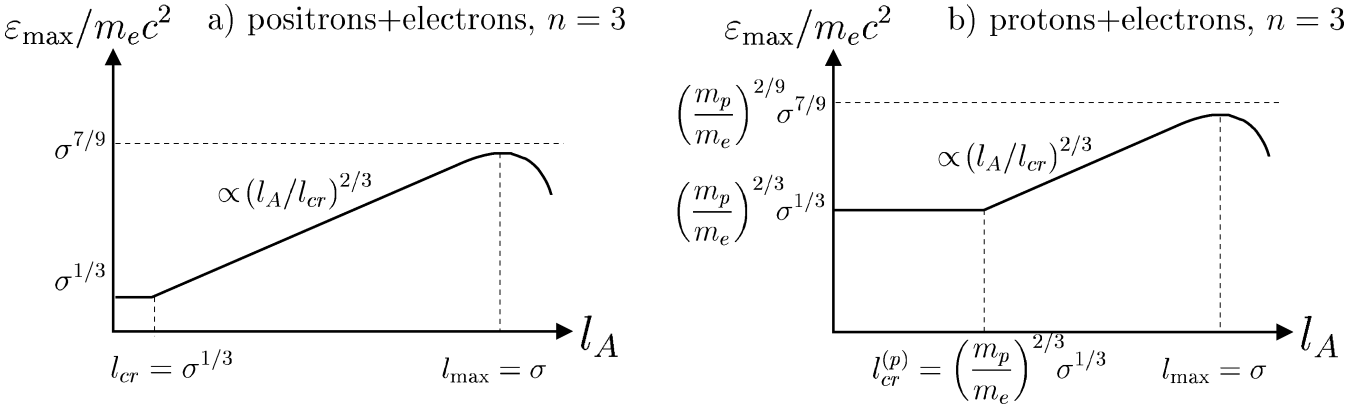

Figure 3. Dependence of the maximum particle energy $\mathcal{E}_{\max}$ on the compactness parameter $l_{\rm A}$ both for electron–proton (a) and electron–positron (b) outflows for $n = 3$. Here $m_{\rm p}$ is a proton mass. The decrease of the particle energy for a very large compactness parameter $l_{\rm A}$ is due to decreasing the total energy flux E_B.

In the Michel magnetization parameter σ (34)

$$\sigma \approx 10^{14}\lambda^{-1}M_9B_4\left(\frac{\Omega R}{c}\right), \tag{118}$$

the main uncertainty comes from the multiplication parameter λ, i.e. in the particle number density n. Indeed, for an electron–positron outflow this value depends on the efficiency of pair creation in the magnetosphere of a black hole, which is still undetermined. In particular, this process depends on the density and energies of the photons in the immediate vicinity of the black hole. As a result, if the hard-photon density is not high, then the multiplication parameter is small ($\lambda \sim$ 10–100; Beskin, Istomin & Pariev 1992; Hirotani & Okamoto 1998). In this case for $(\Omega R/c) \sim 0.1$–0.01 we have $\sigma \sim 10^9$–10^{12}, so that $l_{\rm cr} \sim 10^3$–10^4. On the other hand, if the density of photons with energies $\mathcal{E}_\gamma >$ 1 MeV is high enough, direct particle creation $\gamma + \gamma \rightarrow {\rm e}^+ + {\rm e}^-$ results in an increase in the particle density (Svensson 1984). This gives $\sigma \sim$ 10–10^3, and hence $l_{\rm cr} \sim 10$ for an electron–positron outflow.

From a theoretical point of view, the most interesting result here is the possibility of an additional acceleration of particles outside the fast magnetosonic surface. Indeed, for a high enough photon density ($l_{\rm A} \sim$ 10–100, i.e. for $L \sim 10^{46}$–10^{48} erg s^{-1}) and a small magnetization parameter $\sigma \sim$ 10–100, the compactness parameter $l_{\rm A}$ can exceed the critical value $l_{\rm cr}$ for an electron–positron outflow. In this case, according to Fig. 1(b), our analysis suggests that the kinetic luminosity of the relativistic jet should be proportional to $l_{\rm A}^{2/3} \propto L_{\rm tot}$, where $L_{\rm tot}$ in the total luminosity of the central engine. Kinetic luminosity is not easily determined from observations. However, observational evidence suggests that the radio luminosity of the jets is positively correlated with the luminosity of the central engine and the scatter of this correlation decreases towards larger luminosities (Baum, Zirbel & O'Dea 1995).

For an electron–proton outflow the magnetization parameter (34) can be rewritten in the form (Camenzind 1990)

$$\sigma = \frac{m_{\rm p}}{m_{\rm e}}\left(\frac{\Omega R}{c}\right)^2\frac{B_0^2R^2}{c\dot{M}}$$
$$\approx 3\times 10^4\left(\frac{\Omega R}{c}\right)^2 B_4^2M_9^2\left(\frac{\dot{M}}{0.1{\rm M}_\odot{\rm yr}^{-1}}\right)^{-1}, \tag{119}$$

where $\dot{M} = 4\pi n m_{\rm p}R^2c$ is the mass ejection rate. Hence, for a high ejection rate ($\dot{M} > 0.1\,{\rm M}_\odot$ yr^{-1}) the magnetization parameter $\sigma < m_{\rm p}/m_{\rm e}$. In this case there is no acceleration of plasma. On the other hand, for low ejection rate $\dot{M} < 0.1\,{\rm M}_\odot$ yr^{-1} the magnetization parameter becomes too large for the drag force to be efficient.

Thus, the drag force can only substantially disturb the MHD parameters of a Poynting-dominated outflow either for a very high luminosity of the central engine ($L_{\rm tot} \gg 10^{45}$ erg s^{-1}) or for an electron–positron outflow. In all other cases the action of the drag force remains negligible. In particular, the additional acceleration of particles outside the fast magnetosonic surface is not efficient.

5.2 Cosmological gamma-ray bursts

For cosmological gamma-ray bursts (the central engine is represented by the merger of very rapidly orbiting neutron stars or black holes with $M \sim {\rm M}_\odot$, $R \sim 10^6$ cm, total luminosity $L \sim 10^{52}$ erg s^{-1}, $B_0 \sim 10^{15}$ G; see, e.g., Lee, Wijers & Brown 2000 for details) the compactness parameter $l_{\rm A}$ is extremely large:

$$l_{\rm A} \sim 10^{17}\left(\frac{\Omega R}{c}\right)L_{52}. \tag{120}$$

On the other hand, even for a superstrong magnetic field of $B_0 \sim 10^{15}$ G (which is necessary to explain the total energy release) the magnetization parameter σ is small ($\sigma <$ 1–10), because within this model the magnetic field itself is secondary and its energy density cannot exceed the plasma energy density. Thus, one can conclude that for these characteristics of cosmological gamma-ray bursts the density of photons is very high so that $l_{\rm A} \gg l_{\rm max}$ and the drag force can make it difficult to form a Poynting-dominated outflow. A self-consistent analysis should take into consideration other physical processes such as high optical thickness resulting in the diminishing of the photon density, radiation and particle pressure, etc. Nevertheless, in our opinion, our conclusion may substantially restrict some recent models of cosmological gamma-ray bursts.

5.3 Radio pulsars

For radio pulsars the central engine is a rotating neutron star with $M \sim {\rm M}_\odot$, $R \sim 10^6$ cm, total luminosity of the surface $L_{\rm X} \sim 10^{33}$–10^{37} erg s^{-1} and $B_0 \sim 10^{12}$ G. In this case the magnetization parameter $\sigma \sim 10^4$–10^6, corresponding to relativistic electron–positron plasma, is known with rather high accuracy (see, e.g., Bogovalov 1997). This gives $l_{\rm cr} \sim 10^2$–10^3, and the compactness parameter

$$l_{\rm A} \sim \left(\frac{\Omega R}{c}\right)L_{35} \tag{121}$$

remains small ($<$1) even for the most energetic ($L_{\rm X} \sim 10^{37}$ erg s^{-1}) fast ($\Omega R/c \sim 10^{-2}$) pulsars such as Crab and Vela. Thus, one can conclude that the drag force does not substantially disturb the magnetically dominated outflow from radio pulsars.

Thus, the drag force does not affect the wind characteristics (particle energy, magnetic field structure, etc.) of pulsars. However, interaction of outflowing relativistic particles with thermal photons can be important in other ways. In the wind region ($r \gg R_{\rm L}$) even a weak interaction

with photons can result in a detectable flux of inverse Compton gamma-ray photons (Bogovalov & Aharonian 2000). On the other hand, near the surface of the star ($r \ll R_{\rm L}$), inverse Compton photons are important in the pair creation process (Kardashev, Mitrofanov & Novikov 1984; Zhang & Harding 2000).

ACKNOWLEDGMENTS

The authors are grateful to K. A. Postnov for fruitful discussions. We thank the referee for a detailed report and useful comments. VSB thanks Observatory Paris-Meudon for hospitality. This work was partially supported by the Russian Foundation for Fundamental Research (grant 02-02-16762).

REFERENCES

Baum S.A., Zirbel E.L., O'Dea C.P., 1995, ApJ, 451, 88
Begelman M.C., Li Z.-Y., 1994, ApJ, 426, 269
Begelman M.C., Blandford R.D., Rees M.J., 1984, Rev. Mod. Phys., 56, 255
Beloborodov A.M., 1999, MNRAS, 305, 181
Beskin V.S., 1997, Phys.–Usp., 40(7), 659
Beskin V.S., Okamoto I., 2000, MNRAS, 313, 445
Beskin V.S., Rafikov R.R., 2000, MNRAS, 313, 433 (Paper II)
Beskin V.S., Istomin Ya. N., Pariev V.I., 1992, SvA, 36, 642
Beskin V.S., Kuznetsova I.V., Rafikov R.R., 1998, MNRAS, 299, 341 (Paper I)
Blandford R.D., 2002, in Gilfanov M., Sunyaev R., Churasov E., eds, Lighthouses of the Universe. Springer-Verlag, Berlin, p. 381
Blandford R.D., Znajek R.L., 1977, MNRAS, 179, 433
Bogovalov S.V., 1992, SvA Lett., 18, 337
Bogovalov S.V., 1997, A&A, 327, 662
Bogovalov S.V., 1998, Astron. Lett., 24, 321
Bogovalov S.V., Aharonian F.A., 2000, MNRAS, 313, 504
Camenzind M., 1990, Rev. Mod. Astron., 3, 234
Gabuzda D., Cawtorne T., Roberts D., Wardle J., 1992, ApJ, 338, 40
Gabuzda D., Pushkarev A.B., Cawtorne T., 1999, MNRAS, 307, 725
Hirotani K., Okamoto I., 1998, ApJ, 497, 563
Hirotani K., Iguchi S., Kimura M., Wajima K., 1999, PASJ, 51, 263
Junior W., Biretta J.A., Livio M., 1999, Nat, 401, 891
Kardashev N.S., Mitrofanov I.G., Novikov I.D., 1984, SvA, 28, 651
Kennel C.F., Fujimura F.S., Okamoto I., 1983, Geophys. Astrophys. Fluid Dyn., 26, 147
Lee H.K., Wijers R.A.M.J., Brown G.E., 2000, Phys. Rep., 325, 83
Lery T., Heyvaerts J., Appl S., Norman C.A., 1998, A&A, 337, 603
Li Z.-Y., Begelman M.C., Chiueh T., 1992, ApJ, 384, 567
Melatos A., Melrose D.B., 1996, MNRAS, 279, 1168
Melia F., Königl A., 1989, ApJ, 340, 162
Mézsáros P., Rees M.J., 1997, ApJ, 482, L29
Michel F.C., 1969, ApJ, 158, 727
Michel F.C., 1973, ApJ, 180, L133
Okamoto I., 1999, MNRAS, 307, 253
Phinney E., 1982, MNRAS, 198, 1109
Reynolds C.S., Fabian A.C., Celotti A., Rees M.J., 1996, MNRAS, 283, 873
Sakurai T., 1985, A&A, 152, 121
Sikora M., Madejski G.M., 2000, ApJ, 534, 109
Sikora M., Sol H., Begelman M.C., Madejski G.M., 1996, MNRAS, 280, 781
Svensson R., 1984, MNRAS, 209, 175
Thorne K.S., Price R.H., Macdonald D.A., 1986, Black Holes: the Membrane Paradigm. Yale Univ. Press, New Haven
Tomimatsu A., 1994, PASJ, 46, 123
Turolla R., Nobili L., Calvani M., 1986, ApJ, 303, 573
van Putten M.H.P.M., Levinson A., 2003, ApJ, 584, 937
Zhang B., Harding A.K., 2000, ApJ, 532, 1150

This paper has been typeset from a TEX/LATEX file prepared by the author.